Proposal of a New Scheme Using Extreme Forward Light Scattering for Ion Temperature Measurement in Stellarator and Tokamak Plasmas

A. Gondhalekar and F. Keilmann

IPP 2/2o2
IPP IV/26 August 1971

MAX-PLANCK-INSTITUT FÜR PLASMAPHYSIK
GARCHING BEI MÜNCHEN

MAX-PLANCK-INSTITUT FÜR PLASMAPHYSIK

GARCHING BEI MÜNCHEN

Proposal of a New Scheme Using Extreme Forward Light Scattering for Ion Temperature Measurement in Stellarator and Tokamak Plasmas

A. Gondhalekar and F. Keilmann

IPP 2/202
IPP IV/26 August 1971

Die nachstehende Arbeit wurde im Rahmen des Vertrages zwischen dem Max-Planck-Institut für Plasmaphysik und der Europäischen Atomgemeinschaft über die Zusammenarbeit auf dem Gebiete der Plasmaphysik durchgeführt.

IPP 2/202 A. Gondhalekar
IPP IV/26 F. Keilmann

Proposal of a New Scheme Using Extreme Forward Light Scattering for Ion Temperature Measurement in Stellarator and Tokamak Plasmas.

August 1971 (in English)

Abstract

We propose a measurement of Thomson scattering at an angle of less than one degree. Using a CO_2 laser at $\lambda_o = 10.6\,\mu m$ ensures that $\alpha_e \gg 1$ in a Stellarator or Tokamak-type plasma. The scattered spectrum is then characteristic of the motion of the ions, and the ion temperature can be deduced from its width.

Spectral resolution of the scattered light in the presence of direct light is made possible through a coherent photomixing receiver. Artificially enhanced "false light" serves as local oscillator radiation for the homodyne detection. We describe in detail a setup for measuring ion temperatures up to 1 KeV at plasma densities down to $10^{12}\ cm^{-3}$.

TABLE OF CONTENTS

1. Introduction

Long containment times of plasmas in Stellarator and Tokamak type devices have been achieved. Ion and electron temperatures of o.5 KeV and 1.2 KeV respectively can be reached in a Tokamak /3/ and somewhat lower in a Stellarator plasma. In order to reach fusion conditions, heating of ions is of particular interest, and several heating schemes are being considered.

Of crucial importance to the proper evaluation of these experiments is an unambiquous determination of the ion temperature and, in addition, knowledge of the evolution of the ion velocity distribution function.

2. Methods of Ion Temperature Measurement

Various techniques have been employed to measure the ion temperature in plasmas. All these methods have limited applicability, and often the results are difficult to interpret.

a) Probes

The most important limitation on the use of probes in high energy plasmas is that they contaminate the plasma, and are also destroyed by the plasma. The plasma is disturbed just at the point where the measurement is made. Moreover, the interpretation of probe measurements involves knowledge of the velocity distribution function of the particles /1/. These factors make probe measurements unreliable and their use undesirable.

b) Spectroscopy

The ion temperature measurement by emission spectroscopy employs thermally Doppler broadened radiation from impurity ions. This technique has been applied with Θ-pinch /2/ and Tokamak /3/ plasmas. However, this method depends on the assumption of energy equipartition between different ion species. This may not be accurate, particularly in ion heating experiments in low density plasmas.

c) Particle Methods

The energy distribution of charge exchanged neutrals is related to the ion velocity distribution function /4/. This method has been used to determine the ion temperature in a Tokamak /3/, and in Mirror machines /1o/. At higher temperatures obtained in pinch and plasma focus experiments, neutron emission can be used for this purpose.

d) Thomson Scattering

The spectrum of light scattered from plasma electrons shows, under appropriate conditions, a Doppler broadening characteristic of the ion velocities. This effect, used in conjunction with high power laser light sources, allows a very direct measurement of the ion temperature which does not disturb the plasma. In addition, good temporal and spatial resolution are obtainable /6/.

Since we want to employ this effect, in the following sections we discuss various aspects of Thomson scattering in greater detail. We want, particularly, to show that for the range of parameters in fusion oriented Tokamak and Stellarator devices, a small angle, infrared scattering method has to be developed.

3. Thomson Scattering Theory

The theory of Thomson scattering has been dealt with extensively by various authors, and an excellent review of theory and experiment has been given /6/. We shall here sketch only some of the important conclusions.

Thomson scattering from a plasma occurs due to the interaction of an electromagnetic wave with the plasma electrons. The scattered radiation has a frequency and wave vector spectrum characteristic of the electron density fluctuations.

The geometry of a Thomson scattering experiment is shown in Fig.1. A plane polarised electromagnetic wave with wave vector $\underline{k}_o$ and frequency f_o ($f_o \gg f_{pe}$, the electron plasma frequency) is incident on the plasma. Waves scattered at an angle θ, with wave vector $\underline{k}_s$ and frequency f_s are observed. Scattering occurs from electron density fluctuations of wave vector $\underline{k}$ and frequency f such that

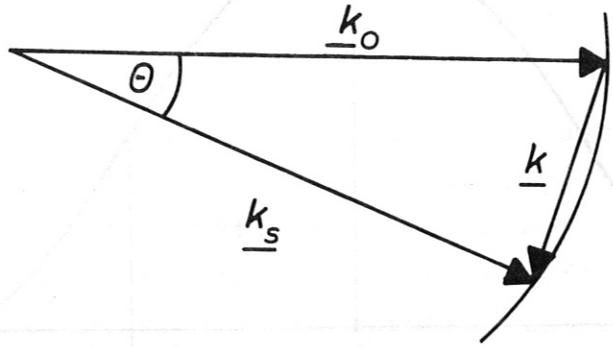

Fig. 1 Geometry of Thomson scattering

$$\underline{k} = \underline{k}_s - \underline{k}_o$$
$$f = f_s - f_o \qquad (1)$$

The frequency spectrum of the scattered light is determined by the parameter

$$\alpha_e = \frac{1}{\lambda_D |\underline{k}|} = \frac{\lambda_o}{\lambda_D \cdot 4\pi \sin\frac{\theta}{2}} \qquad (2)$$

Here, we have assumed that

$$|\underline{k}_s| \simeq |\underline{k}_o|$$

and therefore $$|\underline{k}| \simeq 2|\underline{k}_o| \sin\frac{\theta}{2},$$

θ is the scattering angle, λ_D the Debye length and λ_o the incident wavelength. Three regimes of α_e can be distinguished.

$\underline{\alpha_e \ll 1}$

We obtain incoherent scattering from the plasma electrons, and in the limit $\alpha_e \to o$, the spectrum of the scattered light is just a mapping of the one-dimensional electron velocity distribution function parallel to $\underline{k}$, as shown in Fig.2. The half-width of the spectrum is just the Doppler broadening

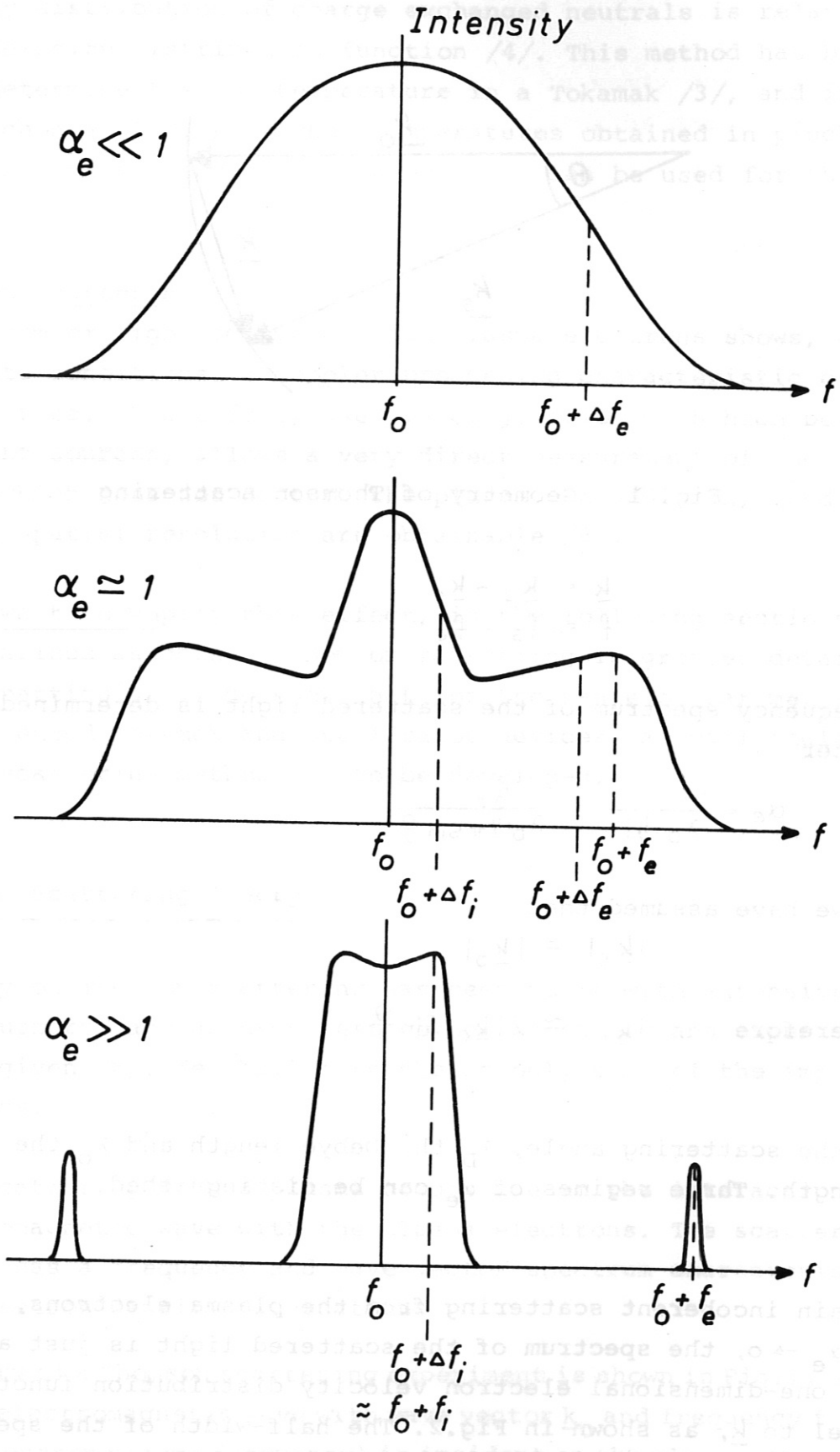

Fig. 2 Variation of the scattered spectrum with α_e, at $T_e = T_i$

$$\Delta f_e = \frac{|\underline{k}|}{2\pi} \cdot v_e \qquad (4)$$

where $v_e = (3\pi T_e/m_e)^{1/2}$ is the thermal velocity of the electrons.

$\underline{\alpha_e \simeq 1}$

As the value of α_e increases, the wavelength associated with the scattering wave-vector $\underline{k}$, that is, physically, the wavelength of the electron density fluctuations being observed, becomes comparable to the Debye length. One then begins to see effects of the collective motions of the electrons, and the spectrum looks as shown in Fig.2. Here, f_e is the frequency of the electron plasma wave,

$$f_e = \left\{ f_{pe}^2 + \frac{|\underline{k}|^2}{4\pi^2} \cdot \frac{3kT_e}{m_e} \right\}^{\frac{1}{2}} \qquad (5)$$

f_{pe} is the electron plasma frequency. For $\alpha_e \simeq 1$ it is possible to determine both the ion and electron temperatures from the same spectrum. The electron temperature can be determined from the position of the electron plasma wave resonance, and the ion temperature from the narrow ion peak at the centre. The width of the ion peak is approximately

$$\Delta f_i = \frac{|\underline{k}|}{2\pi} \left(\frac{3kT_i}{m_i} \right)^{\frac{1}{2}} \qquad (6)$$

Clearly, the experimental spectrum has to be fairly accurately determined to obtain both the ion and electron temperatures.

$\underline{\alpha_e \gg 1}$

This corresponds to the case where the scattering wavelength $\lambda = 2\pi/|\underline{k}|$ is much greater than the Debye length. Then all the collective electron interactions within the plasma show up in the spectrum. First, far out from the central ion feature are the two electron wave resonances at frequency f_e corresponding to the Bohm-Gross longitudinal electron plasma waves (Eq.5).

Second, the central ion feature, which is of particular importance here, appears flat topped. The two slight resonances are at the ion-acoustic wave frequency

$$f_i = \left\{ \frac{f_{pi}^2}{1+\alpha_e^2} + \frac{|\underline{k}|^2}{4\pi^2} \cdot \frac{3KT_i}{m_i} \right\}^{\frac{1}{2}} \qquad (7)$$

The ion temperature can be found from the width of this feature.

From the above equations 4 - 7, we see that for an equilibrium plasma with $T_e = T_i$, we get, for $\alpha_e \ll 1$, $f_e = \Delta f_e$, and for $\alpha_e \gg 1$, $f_i = 1.15\,\Delta f_i$, whereas for $\alpha_e = 1$, we get $f_i = 1.08 \cdot \Delta f_i$ and $f_e = 1.15 \cdot \Delta f_e$.

Now, for $T_i \gg T_e$, the ion acoustic waves are heavily damped, and the central feature gives the one-dimensional ion velocity distribution function parallel to $\underline{k}$ (Fig. 3).

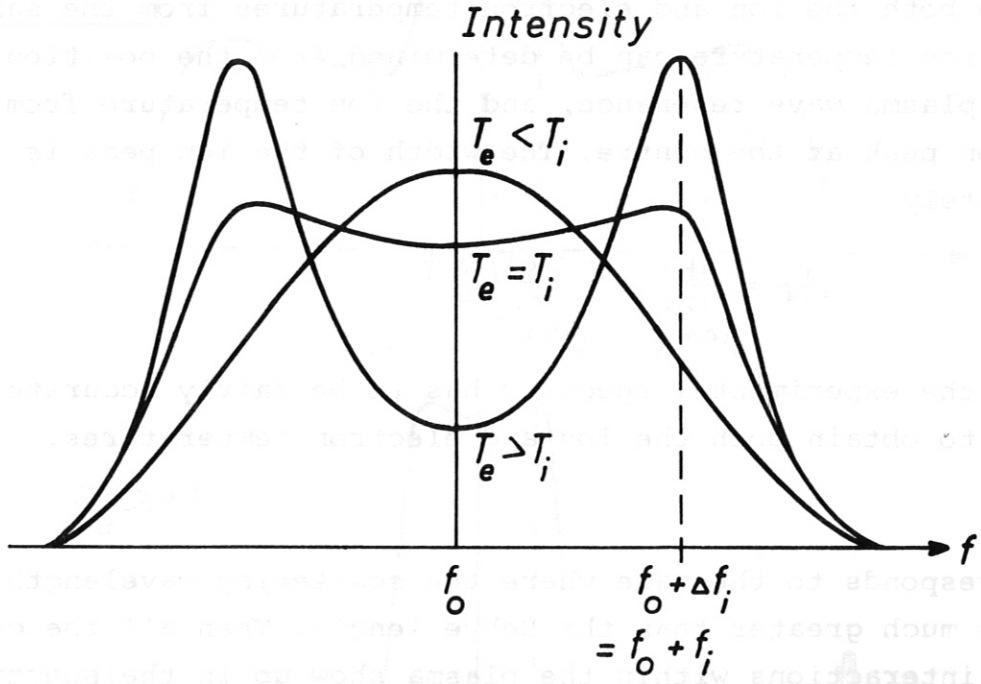

Fig. 3 Ion spectrum for various values of T_e/T_i in the case of $\alpha_e \gg 1$.

When $T_e \gg T_i$ the damping of the ion acoustic waves is small and therefore the two ion resonances can be highly enhanced (Fig. 3).

We take note of other features which may affect the scattered spectrum.

a) Influence of a Magnetic Field

Due to the gyromotion of the particles, the presence of a magnetic field $\underline{B}$ in a plasma affects the shape of the scattered spectrum without altering the total scattered intensity.

In the case of $\underline{k} \perp \underline{B}$, if we first consider $\alpha_e \ll 1$, the spectrum consists of lines located at multiples of the electron gyrofrequency $f_{ce} = \frac{1}{2\pi} \cdot \frac{eB}{m_e \cdot c}$. The envelope is approximately that of the Gaussian profile that would exist in the absence of a magnetic field. This line structure is, however, rapidly smeared out if the angle between $\underline{k}$ and $\underline{B}$ is changed from 90^o. The effect is thus difficult to observe due to aligument problems, but success has recently been reported. Similarly, if $\alpha_e \gg 1$, the ion feature is modulated at the ion cyclotron frequency $f_{ci} = \frac{1}{2\pi} \cdot \frac{eB}{m_i c}$.

If $\underline{k} \parallel \underline{B}$, the presence of the magnetic field has in general no effect on the spectrum. The conditions for the magnetic field to have no effect on the scattered spectrum in case of $\alpha_e \ll 1$ or $\alpha_e \gg 1$ are respectively

$$\cos\phi \gg \frac{f_{ce}}{\Delta f_e} \quad \text{or} \quad \cos\phi \gg \frac{f_{ci}}{\Delta f_i} \tag{8}$$

where ϕ is the angle between $\underline{k}$ and $\underline{B}$.

For very strong magnetic fields, i.e.

$$\frac{f_{ce}}{\Delta f_e} \gg 1 \quad \text{or} \quad \frac{f_{ci}}{\Delta f_i} \gg 1 \tag{9}$$

respectively, the width of the spectrum is contracted by a factor $\cos\phi$ in comparison with the spectrum without a magnetic field.

The case of a weak magnetic field, i.e.

$$\frac{f_{ce}}{\Delta f_e} \lesssim 1 \quad \text{or} \quad \frac{f_{ci}}{\Delta f_i} \lesssim 1 \tag{10a}$$

respectively, is more complicated, but one can say that with the additional criteria

$$\cos\phi \ll \frac{f_{ce}}{\Delta f_e} \ll 1 \quad \text{or} \quad \cos\phi \ll \frac{f_{ci}}{\Delta f_i} \ll 1 \qquad (1ob)$$

respectively, the electron feature shows maxima seperated from each other by the electron gyrofrequency, or the ion feature shows maxima seperated by the ion gyrofrequency.

b) Influence of Collisions

Generally, particle collisions become important for those structures of the scattered spectrum whose frequency is comparable or less than the highest collision frequency. Collisions, however, do not affect the total intensity of the scattered radiation. In the absence of a magnetic field, collisions may be expected to influence most greatly the electron and ion-acoustic plasma resonances. The width and shape of these are both related to the damping rate of the oscillations and hence to the collision frequency. Since the damping of ion-acoustic waves decreases with increasing collision frequency, the ion-acoustic resonance at f_i should be sharpened due to collisions. On the other hand, the electron plasma resonance is broadened by collisions, as the damping of electron plasma waves increases with increasing collision frequency.

d) Influence of Impurities

The addition to a plasma of a small amount of impurities in the form of ions of relatively high charge and mass compared to the charge and mass of the plasma ions can bring about a striking change in the amplitude and frequency distribution of the collective electron density fluctuations, and therefore in the spectrum of scattered light for $\alpha_e \gg 1$ /7/. The effect of the impurity is to alter the scattered spectrum by the addition of a central feature, symmetric about the laser frequency, whose width, compared to that of the pure plasma ion spectrum, is in the ratio of the thermal velocities of the two sorts of ions. The amplitude of this feature depends upon the charge and abundance of the impurity ions.

4. Practical Limitations on Thomson Scattering for Ion Temperature Measurement

Limitations on Thomson scattering for ion temperature measurement can be physical or technical in nature.

To measure the ion temperature, α_e has to be much greater than one. From Eq.2 we see that for a given plasma, this condition can be achieved by either going to long enough wavelengths, or by making the scattering angle θ small enough. We shall consider these two possibilities separately.

Going to long wavelengths, it is immediately obvious that we cannot choose a wavelength near to or greater than the plasma cut-off wavelength. For plasmas of density 10^{12} to 10^{14} cm^{-3} the critical wavelength is 3 cm to o.3 cm. Thus we are limited to working with millimeter or submillimeter waves. However, new problems might arise in this wavelength region due to the presence of randomly moving gross density inhomogeneities. These can introduce further frequency components in the scattered spectrum, in addition to bending the light path.

In the following we consider the range of application of visible and near infrared light. Very small scattering angles θ are now necessary in order to obtain $\alpha_e \gtrsim 1$.

An ultimate limit is imposed on θ by the divergence angle of the input beam. The divergence angle is a measure of the uncertainty in the direction of the beam. Ideally, this can be as low as $\pm \lambda_o/D$, D being the beam diameter. So a reasonable minimum scattering angle should be about three times larger, $\theta \gtrsim 3 \cdot \lambda_o/D$. If a spatial resolution (D) of 1 cm is acceptable, one finds for ruby laser light (λ_o = 6943 Å) $\theta \gtrsim$ o.2 mrad. With existing ruby lasers, however, the diffraction limited divergence can not be reached by a factor 2o, giving us a limit of $\theta \gtrsim 4$ mrad. The range of plasma parameters then accessible for ion temperature measurement with a ruby laser is given by Fig. 4.

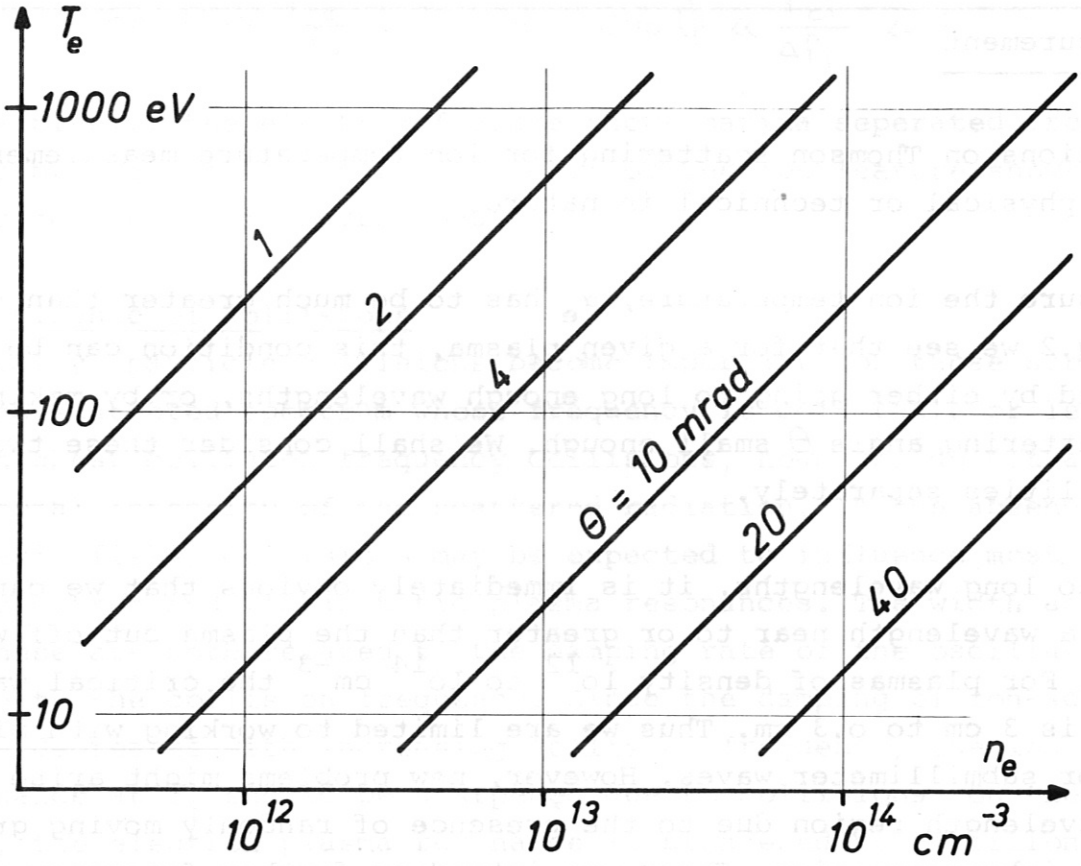

Fig. 4 Plasma conditions for obtaining $\alpha_e = 1$ using ruby laser light at various scattering angles θ.

In practice it seems very unlikely that an experiment at such a small scattering angle could succeed. One drawback is that at very small angles, only a very small solid angle of observation is available, so that the light power gathered may be too small to be detected.

To proceed further in the discussion of practical limits imposed on small angle scattering, we must take into account the particular receiving method used.

a) Photon-Counting Reception

Hitherto, in all light scattering experiments for plasma diagnostics, photon counting techniques have been employed. The essential point here is that the detector as such counts incoming photons, irrespective of their wavelength, thereby destroying the wavelength

information. Therefore, to decode the information, an appropriate narrow-band optical filter is necessary. However, good enough filters are not available if a large amount of false light is present. This is always the case in very small angle scattering experiments, even if we ignore, for the moment, the light scattered at imperfections in the optical components. This is because light intensity comparable to the Thomson scattered light is emitted by the laser source, due to diffraction, at angles much larger than the divergence angle.

The Thomson scattered power for the plasma densities we are interested in is about 15 orders of magnitude below the incident power. On the other hand, if the intensity profile of the laser beam is assumed to be Gaussian, with a divergence angle at half power equal to ε, then the false light is down by 15 orders of magnitude at an angle of about $7 \cdot \varepsilon$, or by 10 orders of magnitude at about $6 \cdot \varepsilon$. So even if a filter rejection ratio of 10^5 could technically be realised, the minimum angle for ruby light scattering comes out to be $\theta \gtrsim 25$ mrad corresponding to 1.43°.

It is interesting to consider whether these numbers change with wavelength. For the case of CO_2 laser radiation at 10.6 μm we have an increase in wavelength by a factor of about 15. However, a practically pure mode can be achieved. So again we get a minimum scattering angle of about 20 mrad. Note that now a 15 fold value of α_e is obtained at the same scattering angle, due to the longer wavelength. The range of plasma parameters thus accessible for ion temperature determination in a CO_2 laser photon-counting scattering experiment is now given by Fig. 5. Although these results are in favour of the feasibility of very small angle CO_2 laser scattering, a technical problem destroys all hopes. This is the relatively high noise power of infrared detectors, which is much larger than the signal power available in small-angle Thomson scattering experiments in the plasmas of interest.

In conclusion, the desired aim of ion temperature determination is not reachable with photon-counting techniques, the reason being an unacceptable signal-to-noise ratio, owing to false light in the visible, and to excessive internal detector noise in the infrared regions.

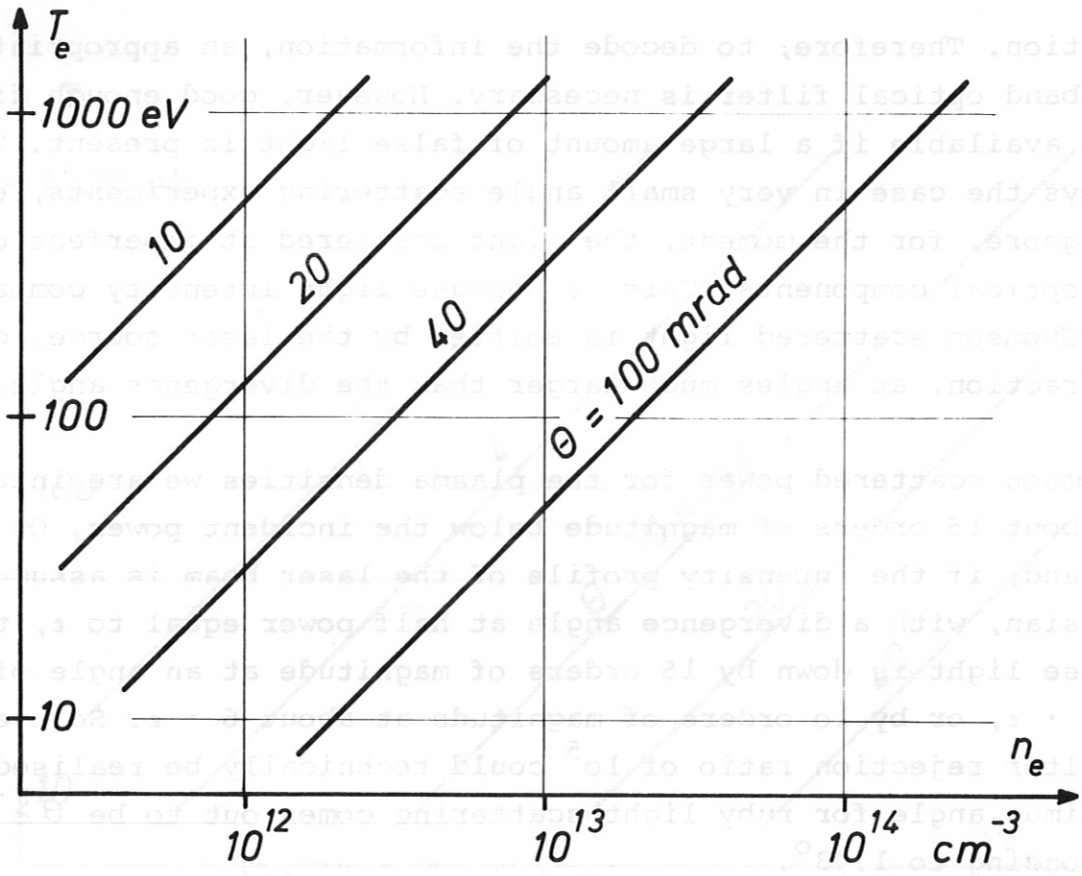

Fig. 5 Plasma conditions for obtaining $\alpha_e = 1$ using CO_2 laser light at various scattering angles

b) Photomixing Reception

A superior technique, known widely in the microwave field, is the receiving scheme of mixing (Fig. 6). This has not been employed until

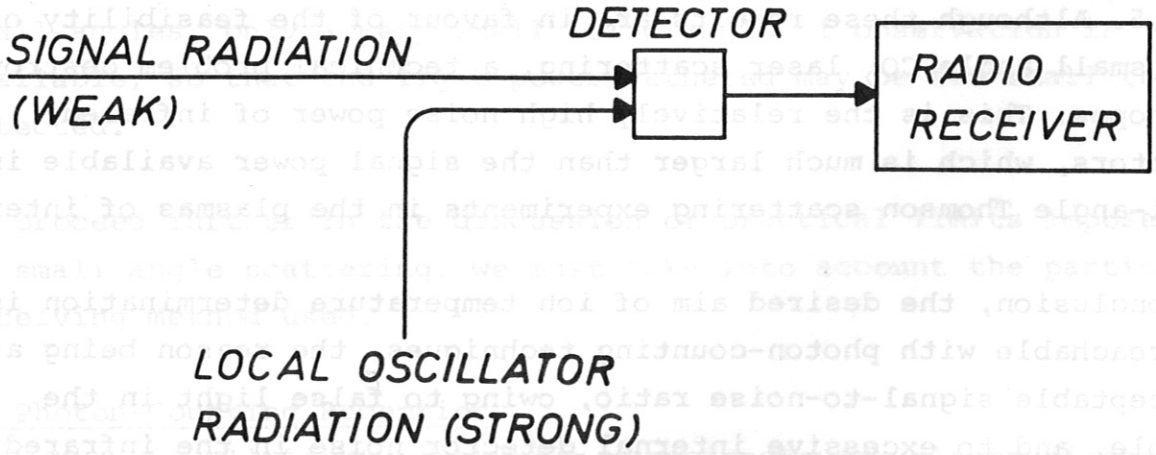

Fig. 6 Principle of photomixing reception

now in plasma scattering experiments with visible or infrared light. We want to show that with this method the limits of false light as well as of internal detector noise can easily be overcome. Photomixing is the optical analogue of radiofrequency heterodyning. It is a form of coherent detection, whereas direct photon counting can be regarded as noncoherent detection. Photomixing in a pure square-law detector can occur because the output photocurrent i is related to the input light power P by

$$i = P \cdot \frac{\eta \cdot e}{h \cdot f} \tag{11}$$

Here η is the quantum efficiency of the detector, e is the electronic charge and hf is the energy of a photon.

Since the light power is proportional to the square of the incident electric field, beat frequency detector currents appear if the incident field is composed of two fields at different frequencies f_S and f_{LO}

$$i = i_S + i_{LO} + 2 (i_S \cdot i_{LO})^{\frac{1}{2}} \cos 2\pi (f_S - f_{LO}) t \tag{12}$$

The subscripts S and LO refer to signal and local oscillator radiation respectively. The first two terms contain current oscillations at the optical frequencies $2f_S$ and $2f_{LO}$; since most detectors have only a relatively slow response, these terms give only a d.c. current. The third term represents a current oscillating at the difference frequency of the two optical fields. The amplitude of this is proportional to $2(P_{LO} \cdot P_S)^{1/2}$. From this we see that with a high power local oscillator the signal current is amplified by a conversion gain $2(P_{LO}/P_S)^{1/2}$, which can be many orders of magnitude.

Much more important than gain in photomixing is the possibility of discrimination against background and internal detector noise. This property is made clear by considering the signal-to-noise power ratio /8/

$$\left(\frac{S}{N}\right)_M = \frac{2 i_S i_{LO}}{i_N^2} \tag{13}$$

Here i_N^2 is the total noise power due to the different noise sources

$$i_N^2 = 2e \cdot \Delta f \cdot (i_D + i_B + i_S + i_{LO}) \tag{14}$$

Δf is the bandwidth of the electronics following the detector; i_D is the detector dark current and i_B is a current due to background radiation falling on the detector.

If now the local oscillator power and therefore i_{LO} can be made large enough, the noise expression (13) for photomixing reduces assymptotically to

$$\left(\frac{S}{N}\right)_M = \frac{i_S}{e \cdot \Delta f} \tag{15}$$

Thus, in the detector output, only the noise inherent in the signal radiation is present.

In contrast, for photon counting detection, the signal-to-noise power ratio is /8/

$$\left(\frac{S}{N}\right)_C = \frac{i_S^2}{i_N^2} \tag{16}$$

where now Eq. 14 reduces to

$$i_N^2 = 2e \cdot \Delta f \, (i_D + i_B + i_S) \tag{17}$$

From Eqs. 15 and 16, we can compare the signal-to-noise power ratios for the two detection schemes. We get

$$\frac{(S/N)_M}{(S/N)_C} = \frac{2 \cdot (i_D + i_B + i_S)}{i_S} \tag{18}$$

For an ideal case where dark current and background radiation can be neglected, we see that the mixing technique results only in a factor of two improvement in S/N.

However, using infrared radiation at low signal powers, this ratio (Eq. 18) can be several orders of magnitude due to the large dark current in available detectors.

In designing a photomixing receiver, great attention has to be given to stringent requirements of wavefront alignment. It is necessary that

the two superimposed fields are aligned throughout the sensitive volume of the detector. This problem becomes more severe at shorter wavelengths.

Apart from internal detector noise, we have seen that false light is a major limit in forward scattering experiments using photon counting detection. But for photomixing, false light no more causes any problems because it only zero-beats with the local oscillator light. Even a very large zero frequency contribution in the difference frequency spectrum can be effectively discriminated against in radio frequency analyzers.

In conclusion, in photomixing detection, although the detector sees a wide range of frequencies, the spectral information is not lost in the detector; but due to the coherent nature of detection, the spectral information is transferred to the radio frequency domain where it can be efficiently decoded.

5. Proposed Extreme Forward Scattering Method Employing a CO_2 Laser and Homodyne Spectrum Detection

Here we propose a new scheme to measure the ion temperature, in a Stellarator or Tokamak plasma, by extreme forward scattering of CO_2 laser radiation at a wavelength of lo.6 μm.

We choose the angle of scattering to be of the order of a few milliradians. At such a small angle the scattered spectrum has a form from which the ion temperature can be deduced; furthermore, the scattered spectrum is narrow enough ($\Delta f_i \approx$ loo MHz), so that it can be detected with a common infrared detector (risetime 3 nsec), amplified in a UHF receiver and either displayed directly, or further spectrum-analyzed.

The transversely excited atmospheric pressure CO_2 laser can easily deliver a long enough pulse (1 μsec), so that the UHF modulation can be resolved. The power available (2 MW) allows an acceptable signal-to-noise ratio. Because of the very small scattered power (lo^{-lo}W) the adaption of such a coherent receiving technique is the only possible way of resolving the spectrum.

Extremely good use can now be made of the "false light" originating at optical imperfections in windows. This light is not shifted in frequency and can serve therefore as local oscillator radiation, thus amplifying the Thomson scattered signal.

The details of the proposed method are discussed in the next section. A schematic setup is shown in Fig. 7.

A CO_2 laser beam of diameter 5 mm is directed into the plasma. It enters and leaves the plasma chamber through Brewster angle windows. Scattered light arises due to Thomson scattering by the plasma (signal radiation) and due to scattering at imperfections in the windows (local oscillator radiation). The latter can be enhanced by an additional scatter plate, if necessary.

At a distance of 3 m from the plasma, the direct beam is blocked by a shield 4 cm in diameter, whereas the scattered light is collected by a lens with an aperture of 8 cm, and a focal length of 5o cm. The lens produces an image of the plasma which is demagnified by a factor of 5. The image is produced on a liquid nitrogen cooled HgCdTe-detector having a diameter of 1 mm. In order that light scattered at a preselected angle only, e.g. $1^o \pm 1$ mrad, is used for this imaging, a field stop of appropriate annular form is placed in the focal plane of the lens. The detector is equipped with a filter cooled to 77 ^oK, thus effectively reducing the thermal background radiation and also the plasma radiation.

The detector signal is amplified and either analyzed in an electronic spectrum analyzer, or alternatively, it can be recorded and analyzed in a computer. The ion temperature is determined from the shape of the spectrum. If a sufficient resolution of the radio frequency signal can be achieved, the ion line profile can also yield information on the electron temperature, the magnetic field strength, the effective collision frequency and deviations in the ion velocity distribution from equilibrium. No absolute radiation intensity measurements are involved.

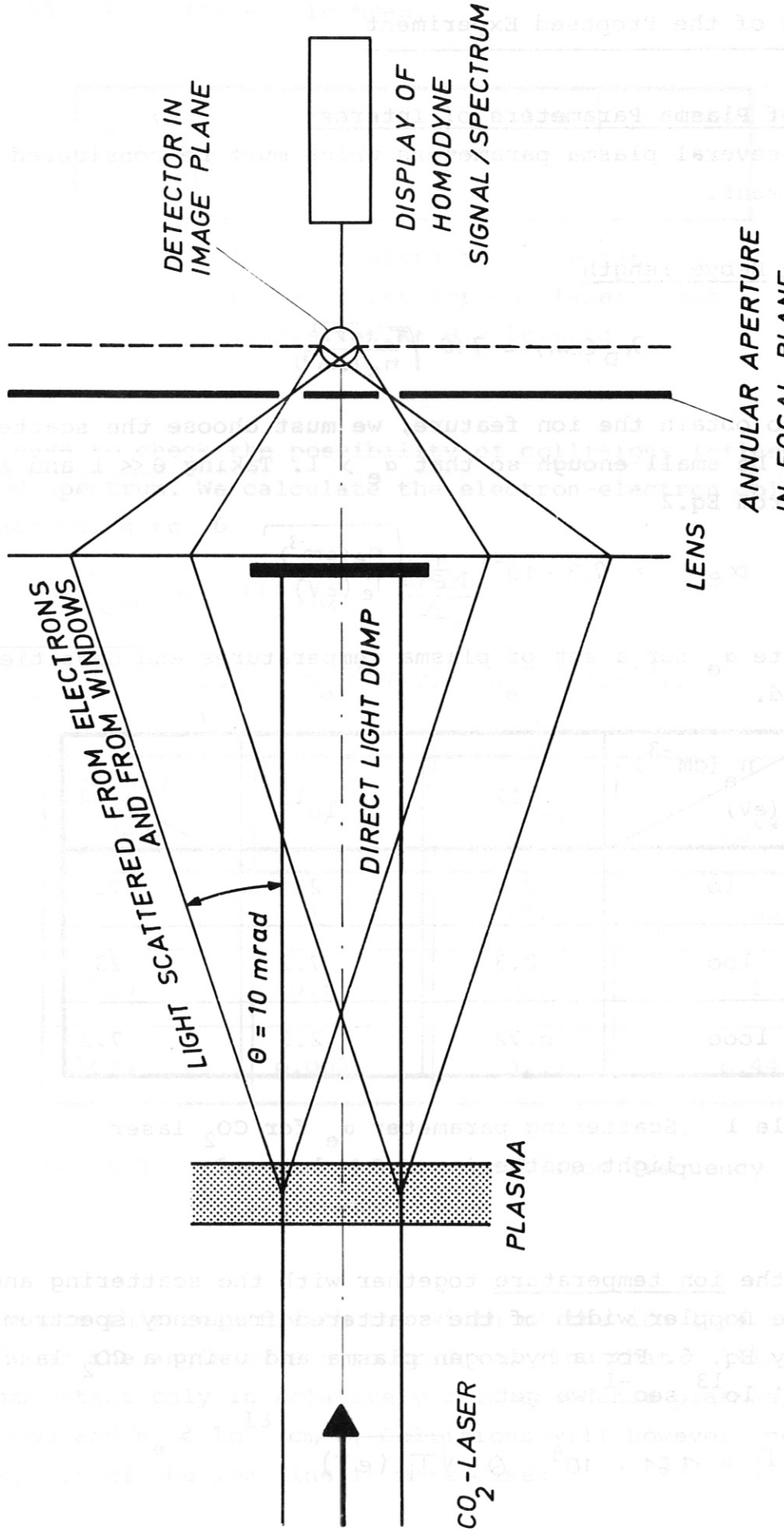

Fig. 7 Scheme of the proposed forward scattering experiment

6. Details of the Proposed Experiment

a) Range of Plasma Parameters of Interest

There are several plasma parameters which must be considered in planning the experiment.

One is the Debye length

$$\lambda_D (cm) = 740 \sqrt{\frac{T_e (eV)}{n_e (cm^{-3})}} \qquad (19)$$

In order to obtain the ion feature, we must choose the scattering angle θ to be small enough so that $\alpha_e > 1$. Taking $\theta \ll 1$ and $\lambda = 10.6\,\mu m$, we have, from Eq.2

$$\alpha_e = 2.3 \cdot 10^{-7} \cdot \frac{1}{\theta} \sqrt{\frac{n_e (cm^{-3})}{T_e (eV)}} \qquad (20)$$

We calculate α_e for a set of plasma temperatures and densities, using $\theta = 10$ mrad.

T_e (eV) \ n_e (cm^{-3})	10^{12}	10^{13}	10^{14}
10	7.2	23	72
100	2.3	7.2	23
1000	0.72	2.3	7.2

Table 1 Scattering parameter α_e for CO_2 laser light scattering at $\theta = 10$ mrad

Secondly, the ion temperature together with the scattering angle θ defines the Doppler width of the scattered frequency spectrum. This is given by Eq. 6. For a hydrogen plasma and using a CO_2 laser with $f_o = 2.83 \cdot 10^{13}\ sec^{-1}$ we get

$$\Delta f_i = 1.61 \cdot 10^9 \cdot \theta \cdot \sqrt{T_i (eV)} \qquad (21)$$

This is calculated for Θ = 1o mrad.

T_i (eV)	1o	1oo	1ooo
Δf_i (MHz)	51	16o	51o

Table 2 Ion line width at different ion temperatures for CO_2 laser light scattering at Θ = 1o mrad

Next we have to check the possibility of collisions influencing the scattered spectrum. We calculate the electron-electron collision frequency according to /6/

$$f_{coll} = 1.33 \cdot f_{pe} \cdot \frac{\ln \Lambda_o}{\Lambda_o} \qquad (22)$$

where $\Lambda_o = 1.55 \cdot 1o^{1o} \cdot T_e^{3/2}(eV) \cdot n_e^{-1/2}(cm^{-3})$.

T_e (eV) \ n_e (cm^{-3})	$1o^{12}$	$1o^{13}$	$1o^{14}$
1o	3.2	19.2	265
1oo	o.13	1.2	11
1ooo	o.oo5	o.o5	o.44

Table 3 Electron-electron collision frequency f_{coll} in MHz

If we compare this result with the width of the ion line to be measured, at the angle of Θ = 1o mrad, we find that collision effects become important only in relatively cold and dense plasmas, with $T_e \lesssim$ 1o eV and $n_e \gtrsim 1o^{13}$ cm^{-3}. Collisions will, however, smear out finer details of the ion line in more cases.

Let us now consider the possible magnetic field modulation of the ion line. In the scattered spectrum, maxima can show up seperated by the ion gyrofrequency, which for hydrogen ions in a lo kGauss field is 15.3 MHz. The total power of the scattered light is, however, not altered by the magnetic field. The magnetic field modulation is only detectable if the collision frequency is small enough, and, in an extreme forward scattering experiment (Eqs. 8 - lo), if the beam direction is parallel to the magnetic field. The latter condition is well fulfilled over a considerable path length if the probing laser beam traverses a toroidal plasma tangential to its major perimeter.

With the homodyne method being proposed, a resolution of the magnetic field modulation seems within reach. Therefore, together with the ion temperature, we have the possibility of gaining information about the magnetic field in the plasma. With a choice of a suitable scattering geometry this method could be extended to investigate poloidal magnetic fields in Stellarator or Tokamak plasmas.

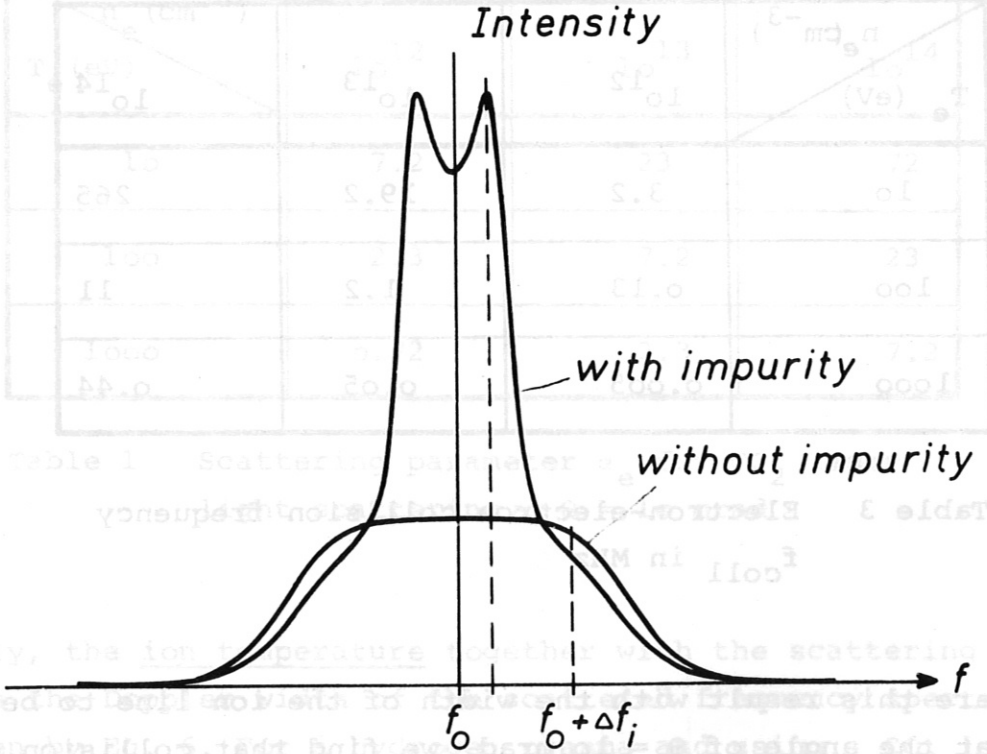

Fig. 8 Effect on the ion spectrum of 5 % oxygen impurity ions in a fully ionized hydrogen plasma

Lastly the presence of heavy ion impurities in Stellarator and Tokamak plasmas will substantially affect the shape of the scattered spectrum. As an illustration, we take the impurity content found in the Princeton ST Tokamak /3/, which is about 5 % of oxygen. Following /7/ we calculate the spectra as shown in Fig. 8. With the impurities, there arises an additional peak symmetric about the center frequency. The width of this peak, characteristic of the thermal motion of the oxygen ion, is now a factor of $\sqrt{16}$ smaller than Δf_i. Therefore, the ion temperature measurement will not be affected in such a case.

b) Scattered Signal Radiation

To achieve complete mixing of signal and local oscillator light, both beams must be coherent over the detector surface. As regards the Thomson scattered signal light, this is easily achieved by using a fundamental mode laser beam.

Both beams should also have the same polarizations. This presents no difficulty, because no polarization change has to be considered in small-angle Thomson scattering.

The power differential cross section of an electron for scattering into a small solid angle element $d\Omega$ around the scattering angle Θ is

$$d\sigma\ (cm^2) = 0.794 \cdot 10^{-25}\ \cos^2\Theta\ d\Omega \qquad (23)$$

For forward scattering this reduces to

$$d\sigma\ (cm^2) = 0.794 \cdot 10^{-25}\ d\Omega \qquad (24)$$

We collect light scattered into a conical shell around the incident beams axis. This is bounded by the small angles Θ_{max} and Θ_{min}. Defining $\alpha = 0.5\ (\Theta_{max} + \Theta_{min})$ and $\beta = 0.5\ (\Theta_{max} - \Theta_{min})$ we can write for the solid angle

$$\Omega = 4\pi\alpha\beta \qquad (25)$$

Thus the signal power cross section of an electron is

$$\sigma\ (cm^2) = 10^{-24}\ \alpha\beta \qquad (26)$$

To calculate the signal power due to all electrons in the scattering volume, we assume that we can add the individual signal powers from each electron. However, in observing the ion feature, with $\alpha_e \gg 1$, the effective scattering cross-section of an electron in a hydrogen plasma (Z = 1) and $T_e/T_i = 1$ is just half the Thomson cross-section.

For the active volume in an extreme forward scattering experiment we must use the beam cross section multiplied by the interaction length L within the plasma. The signal power P_S is related to the laser power P_L by

$$P_S = P_L \cdot n_e \cdot L \cdot \sigma/2 \qquad (27)$$

As an example, we calculate the lower limit of P_S putting $n_e = 10^{12}\ cm^{-3}$. Assuming practical values $P_L = 2 \times 10^6$ W, L = 25 cm, α = 10 mrad and β = 1 mrad, we obtain $P_S = 2.5 \cdot 10^{-10}$ W.

This means that at least 13 signal photons arrive at the detector in each time interval of 1 nsec.

c) Local Oscillator Radiation

As stated above, the local oscillator radiation must be applied coherently with the signal radiation on the detector; this means that the polarizations and the wavefronts of both beams have to match.

The frequency spread of the local oscillator radiation has to be smaller than the width of the smallest structures one wishes to resolve in the scattered spectrum.

The local oscillator power should be large enough to give optimum heterodyne output, but it must be smaller than the saturation limit of the detector. In practice, we use about 1 mW of local oscillator power, giving a conversion gain of $2(P_{LO}/P_S)^{1/2} \approx 4000$.

The normal method of supplying l.o. power for mixing is by a seperate, stable light source. In this configuration, using optical or infrared light, alignment of the two wavefronts is very difficult. Furthermore, the advantage of setting the l.o. frequency apart from the center of the scattered frequencies can not really be made use of because the response time of available detectors is limited to about 1 nsec. Thus we are restricted to a homodyne receiving system.

Now the local oscillator radiation can be derived from the same laser beam as that used for scattering. A great advantage here is that shifts in the laser frequency f_o during the pulse (chirping) do not affect the beat spectrum, if the difference between the path length of the two beams is short enough. This imposes another restriction on the optical setup.

A new idea here rescues us from the alignment problems. We introduce a way of using the same light path for both signal and l.o. radiation. At the very small scattering angle that we employ, we can take for the local oscillator the light in the wings of the angular intensity distribution of the direct laser beam, normally looked upon as false light. At scattering angles much larger than the laser divergence angle, artifical enhancing of the false light is necessary to supply sufficient l.o. power. This can be done with a scatter plate which should be placed near the scattering plasma, so that matching of the wave fronts at the detector is achieved.

d) Background Radiation

At the wavelength considered (lo μm) filters are available with a bandwidth of o.ol μm. We calculate the radiation falling on the detector within this passband, which is emitted by the plasma and by the 3oo ^{o}K background. The filter is assumed to be inside the detector dewar at 77 ^{o}K.

We can estimate the plasma emissivity at lo μm to be very small, since we consider densities very much smaller than the critical density $n_e = 10^{19}$ cm^{-3} appropriate to lo μm. Therefore we neglect reabsorption. The emitted radiation is purely bremsstrahlung, since recombination or line radiation is not present. In hydrogen we obtain

$$I\,(W/cm^3) = 1.9\cdot 10^{-36}\cdot \frac{n_e^2\,(cm^{-3})}{T_e^{\frac{1}{2}}\,(eV)}\cdot \frac{\Delta\lambda\,(cm)}{\lambda^2\,(cm)}\cdot e^{-1.24\cdot 10^{-4}/\lambda\,(cm)\cdot T_e\,(eV)} \qquad (28)$$

In this context, inserting $n_e = 10^{14}$ cm^{-3} and $T_e = 10$ eV as the extreme conditions from our range of plasma parameters, we get $5.6 \cdot 10^{-9}$ W/cm^3 as an upper limit for the plasma radiation power. As we use a solid angle of $1.3 \cdot 10^{-4}$ and an effective volume of at most 1000 cm^3, we find for the maximum possible plasma radiation level $0.6 \cdot 10^{-10}$ W.

For an estimate of the 300 ^{o}K background radiation we use Planck's formula

$$I\,(W/cm^2) = 1.2\cdot 10^{-12}\cdot \frac{\Delta\lambda}{\lambda}\cdot \frac{1}{\lambda^4\,(cm)}\cdot \frac{1}{e^{\frac{1.439}{\lambda\,(cm)\cdot T_e\,(eV)}} - 1} \qquad (29)$$

obtaining 10^{-5} W/cm^2 sterad. With the field of view of 5^{o} (.024 sterad) and the detector area of 1 mm^2 this gives $2.4\cdot 10^{-9}$ W. This, however, can be reduced by orders of magnitude, if the emittance of the bodies in the field of view of the detector is made small.

We conclude that the background radiation power will at worst just be equal to the scattered signal power.

e) Noise Considerations

The signal at the output of the photoconductive detector in a homodyne receiver consists of a fluctuating current lasting for as long as the CO_2 laser pulse, τ_L. It contains spectral components from τ_L^{-1} up to, depending on the ion temperature, between 50 and 500 MHz. As there is no signal information at frequencies below τ_L^{-1}, it will be practical to employ an appropriate high-pass filter, in our case at 1 MHz, in the signal preamplifier. Therefore, we need not care about d.c. background or plasma radiation levels. However, we have to find out the fluctuations in these radiation sources, as well as in the local oscillator, occurring at frequencies between 1 and 500 MHz.

First we want to consider the fluctuations in the scattered signal radiation. If n is the number of photons received during the integration time of interest, then this number will fluctuate due to photon statistics. If $\bar{n}$ is the mean value of n, then we can define $\Delta n = n - \bar{n}$ as the statistical deviation. The standard deviation comes out to be $\sqrt{\overline{(\Delta n)^2}} = \sqrt{\bar{n}}$. To decode the homodyne frequency spectrum, we know from the sampling theorem that two samples are necessary per period of the highest frequency of interest. Therefore we have as an integration time not more than 1 nsec. As was estimated above, in the worst case we still get 13 signal photons at the detector per nsec. So with a noise-free detector we expect a signal-to-noise power ratio of at least $S/N = 13\eta$, where η is the quantum efficiency of the detector.

As for the background radiation noise, the signal-to-noise power ratio is given /8/ by $S/N = n_s^2/2n_b\Delta f$, where n_s and n_b are the numbers per second of signal and background photons respectively. Δf is the receiver bandwidth, here 500 MHz. We use, from the preceding sections, $n_s = 1.3 \cdot 10^{10}\ \mathrm{sec}^{-1}$ and $n_b \leq 1.3 \cdot 10^{10}\ \mathrm{sec}^{-1}$, and obtain $S/N \geq 13$ due to background radiation.

However, through the mixing process, a strong discrimination is achieved against the background radiation noise, as well as against internal detector noise (Eq. 15). Thus, in the detector output, the signal-to-noise power ratio is given only by that of the input signal. A gain of a factor of two in S/N is achieved through the mixing (Eq. 18), so in the end we get $S/N = 26\eta$.

f) Detector

To detect the homodyne scattering signal in the proposed experiment, the time constant of the detector has to be small, preferably 1 nsec or less.

Secondly, the detectivity as well as the linear response range must be large enough to guarantee a noise-free-detection of the beat spectrum. But there is no need for us to calculate the minimum values required for these detector properties for our experiment. Instead we take well established results for the performance of photoconductive detectors at 10 µm wavelength /9/. The heterodyne response of the

HgCdTe-detector was found to be within a factor of two in S/N compared to the ideal one. For S/N = 1, a signal power $7 \cdot 10^{-20}$ W in a 1 Hz bandwidth was shown to be necessary.

Such a detector is available with 400 MHz bandwidth, together with a quantum efficiency of 20 %. Thus on proper adjustment of the local oscillator power a S/N larger than 2 will be obtained even at the low electron density of 10^{12} cm^{-3} in the proposed experiment.

The local oscillator power used in /9/ with the HgCdTe detector was about 1 mW. The responsitivity being of the order of 200 V/W, we can expect for a scattered signal power of $2.5 \cdot 10^{-10}$ W an r.m.s. signal voltage of 0.2 mV.

g) CO_2 Laser

We propose using a TEA-CO_2 laser as a light source. For a sufficient definition of the scattering angle, we require the divergence of the laser beam in the scattering region to be less than about 2 mrad. For a fundamental mode at $\lambda = 10.6$ µm we find, for a beam waist diameter of 0.5 cm, a full far-field divergence angle of 2.66 mrad / 5 /. The corresponding near-field distance is 3.75 m. If the beam waist is arranged to be in the scattering region, the length of which (30 cm) is much shorter than 3.75 m, then the full beam divergence angle there is at most 0.24 mrad. Therefore, some deterioration of the laser beam as compared to the ideal mode can be tolerated.

However, the laser must be guaranteed to oscillate in a single transverse and longitudinal mode. Otherwise, false beats arise in the scattered signal. The unwanted modes can be suppressed by a proper choice of the laser cavity and by using a Fabry-Perot mode selector. For example, if the Fabry-Perot cavity is built with two mirros 6 cm apart, a longitudinal mode distance of 2.5 GHz results, whereas the fluorescence line width of the laser is about 4 GHz. Since both signal and local oscillator radiation come from the same laser the exact frequency within the fluorescence line width is of no importance.

A laser power of about 2 MW is required to achieve S/N > 1.

Normally, the pulse length is of the order of 0.3 µsec, which is long enough for a resolution of the desired beat frequencies. However, more information can be achieved by tailoring the laser pulse length to a few µsec, which is possible.

It is necessary that the laser output occurs at a single rotational transition, not because of false beats which would be at multiples

of 55 GHz, but because of the narrow bandpass of the filter at the detector (o.ol /um = 28 GHz). A chirping of the laser frequency during the pulse, if it occurs, can not be greater than 4 GHz. As this is very much smaller than the laser frequency, 283oo GHz, chirping can not deteriorate the scattering beat spectrum.

h) Receiver Optics

In heterodyne communication receivers employing infrared radiation the local oscillator radiation is applied as a plane wave. The signal beam is usually focussed on the detector. Thereby the focal length of the lens must be properly chosen so that the diffraction limited spot diameter (Airy disk) is larger than the detector diameter. This then ensures an approximately plane wave for the signal light also. Note that some signal light power is lost, and also alignment is very critical /8/. An advantage of such an optical system is that the local oscillator frequency can be offset, say by 3 GHz, so that amplification even of a broad-band modulation spectrum is made easy.

As already discussed in Section 5.c, for the proposed experiment we want to use the same light path for both the signal and the local oscillator radiation. This ensures proper alignment of the wavefronts.

The angular selection of the scattered light is done by an annular focal plane aperture. In order to prevent gas breakdown and damage of the diaphragm, we reject most of the direct beam in a preliminary light stop (Fig. 7).

As mentioned above, the laser beam waist of 5 mm diameter is located in the scattering region. We place the receiving lens at 3 m distance. Here the natural divergence has expanded the beam diameter to 1 cm. In order to collect all the light scattered at angles between 9 and 11 mrad, a light stop of at most 4 cm diameter may be employed to intercept the unscattered beam. This light stop could be a mirror inclined at a small angle to the laser beam so as to direct most of the unscattered light into a dump. Furthermore, the lens aperture diameter should be 8 cm, in order to collect all the light we want to use.

The light passing the lens is now focussed at the focal distance of 5o cm. For finally selecting the range of scattering angles an annular

aperture is introduced there. Its inner diameter will now be 9 mm, and the outer diameter 11 mm.

We place the detector in the image plane, where the selected light is best concentrated. The distance of the image plane from the focal plane is 1o cm. The demagnification by the system is 5. Therefore a detector 1 mm wide will collect all the selected signal light.

i) Signal Amplification and Analysis

The output voltage of the detector follows the power pulse form $P_L(t)$ of the laser. If the local oscillator power is 1 mW, and if the detector responsivity is 2oo V/W, this voltage level is 2oo mV. However, only the high frequency fluctuations of this voltage level, with an r.m.s. value of o.2 mV, are further amplified and analyzed.

Since the signal as well as the local oscillator powers vary with $P_L(t)$, the high frequency mixer output voltage is also enveloped by $P_L(t)$.

Following the detector the oscillating voltage is to be amplified by 3o to 8o db, depending on the voltage requirements of the display instrument. This can be a single-scan spectrum analyzer, if the laser pulse is at least a few /usec long. Alternatively, the oscillating voltage can be recorded, and the spectrum can be computed from the recorded trace.

Note that the resulting spectrum of the detector voltage has to be squared to obtain the spectrum of the scattered light power.

j) Smearing of the Spectrum

Limitations to the accuracy of the proposed ion temperature measurement are imposed by various sources of smearing of the spectrum. Here we do not mean the influences of collisions, magnetic fields or impurity ions, since these effects may provide additional information.

Three different factors contribute to a smearing of the spectrum, which in principle can be corrected for by appropriate unfolding procedures:

Variation in the scattering angle. We expect to collect light scattered at angles between 9 and 11 mrad. Thus there is a substantial variation of the scattering angle, leading to some smearing of the frequency spectrum.

Inhomogeneous plasma. Due to the extremely small scattering angles, the scattering plasma volume has to extend over a large length in the beam direction. Thus temperature variations, and under critical conditions, also variations of α_e will give further smearing.

Observation time. The finite observation time given by the laser pulse length τ_L causes a smearing, characterized by $\Delta f = \frac{1}{\tau_L}$.

7. Possible Refinements and Extensions of the Proposed Technique

In the preceding section we have described a specific experimental arrangement optimized to the ion temperature measurement for a range of plasmas covering $10^{12} \lesssim n_e \lesssim 10^{14}$ cm^{-3} and $10 \lesssim T_i \lesssim 1000$ eV. Depending on technical advances an improvement of this setup will be possible. The technique described can also be applied to different experimental aims.

First, if a longer laser pulse becomes available, then lower frequency structures in the spectrum can be investigated. If in this case, however, one is interested only in the half-width of a thermally broadened spectrum, then the scattering angle can be reduced. As this results in a proportional narrowing of the necessary homodyne bandwidth, this relaxes our demands on the radio frequency electronics.

On the other hand, a reduction in scattering angle allows an extension of the method to measuring higher ion temperatures without a change of the detecting bandwidth. This can be essential in situations where the detector bandwidth is already fully used.

An increase in scattering angle may in some cases be necessary where one wants a better spatial resolution in the direction of the laser beam. In this context the possibility of using a laser with longer wavelength should be mentioned. If a powerful HCN laser at $\lambda_o = 337\,\mu$m can be used instead of the CO_2 laser, then the scattering angle can be increased by a factor of 32, while keeping α_e as well as Δf_i constant.

If very small scattering angles are used, then in order to determine the local ion temperature one has to scan through the plasma in the desired cross section and then carry out an Abel-type inversion.

Note that only that component of the ion temperature which is parallel to $\underline{k}$ is measured. In an extreme forward scattering experiment, $\underline{k}$ is always perpendicular to the laser beam. Therefore, by blocking sections of the annular focal plane aperture, any anisotropy of the ion motion can be detected.

The proposed experimental technique can be applied to the study of plasma waves in a range which can not be investigated by microwaves, i.e., plasma waves of relatively small wavelength. The wave frequency has to be within the detector bandwidth. Even waves with higher frequency can be observed, if one adapts a true heterodyne technique. This involves an offset in the frequency of the local oscillator light, which can be achieved by using either a frequency shifter or a seperate laser.

8. Acknowledgments

We are grateful to K. Büchl, A. Salat, M. Tutter and the members of the wave group for very valuable discussions. We also want to thank Mrs. G. Stöckermann for the drawings and Miss C. Wallner for typing the manuscript.

9. References

1 L. Schott in Plasma Diagnostics, Ed. W. Lochte-Holtgreven, p. 668, Amsterdam 1968.

2 A.C. Kolb et al., Paper CN-21/98 IAEA Conference, Culham 1961.

3 D. Dimock, D. Eckartt, H. Eubank, E. Hinnov, L.C. Johnson, and D.J. Grove, Paper CN-28/C-9 IAEA Conference, Madison 1971.

4 H.W. Drawin in Plasma Diagnostics, Ed. W. Lochte-Holtgreven, p. 833, Amsterdam 1968.

5 H. Kogelnik and T. Li, Applied Optics 5, 155o (1966)

6 D.E. Evans and J. Katzenstein, Rep. Prog. Phys. 32, 2o7 (1969).

7 D.E. Evans, Plasma Physics 12, 573 (197o).

8 M. Ross, Laser Receivers, New York 1966.

9 H.W. Mocker, Appl. Optics 8, 677 (1969).

lo W. Bernstein, V.V. Chechkin, L.G. Kuo, E.G. Murphy, M. Petravic, A.C. Riviere, and D.R. Sweetman, Culham Laboratory Report CLM-P91 (1966).